p-Cymene attenuates cancer pain via inhibitory pathways and modulation of calcium currents

Wagner B.R. Santos , Marlange A.O. Melo , Rafael S. Alves , Renan G. de Brito , Thallita K. Rabelo , Lindaura da S. Prado , Virginia K. dos S. Silva , Daniel P. Bezerra , José E.R. de Menezes-Filho , Diego S. Souza , Carla M.L. de Vasconcelos , Luciana Scotti , Marcus Tullius Scotti , Waldecy de Lucca Júnior , Lucindo J. Quintans-Júnior , Adriana G. Guimarães

PII: S0944-7113(18)30281-2
DOI: https://doi.org/10.1016/j.phymed.2019.152836
Article Number: 152836
Reference: PHYMED 152836

To appear in: *Phytomedicine*

Received date: 1 March 2018
Revised date: 10 July 2018
Accepted date: 23 August 2018

Please cite this article as: Wagner B.R. Santos , Marlange A.O. Melo , Rafael S. Alves , Renan G. de Brito , Thallita K. Rabelo , Lindaura da S. Prado , Virginia K. dos S. Silva , Daniel P. Bezerra , José E.R. de Menezes-Filho , Diego S. Souza , Carla M.L. de Vasconcelos , Luciana Scotti , Marcus Tullius Scotti , Waldecy de Lucca Júnior , Lucindo J. Quintans-Júnior , Adriana G. Guimarães , p-Cymene attenuates cancer pain via inhibitory pathways and modulation of calcium currents, *Phytomedicine* (2019), doi: https://doi.org/10.1016/j.phymed.2019.152836

p-Cymene attenuates cancer pain via inhibitory pathways and modulation of calcium currents

Wagner B. R. Santos[a], Marlange A. O. Melo[a], Rafael S. Alves[a], Renan G. de Brito[a], Thallita K. Rabelo[a]; Lindaura da S. Prado[b], Virginia K. dos S. Silva[c], Daniel P. Bezerra[d], José E. R. de Menezes-Filho[a], Diego S. Souza[a], Carla M. L. de Vasconcelos[a], Luciana Scotti[e], Marcus Tullius Scotti[e], Waldecy de Lucca Júnior[f], Lucindo J. Quintans-Júnior[a], Adriana G. Guimarães[g,*]

[a]Department of Physiology, [f]Department of Morphology, Federal University of Sergipe, São Cristóvão, SE, Brazil

[b]Postgraduate program in sciences applied to health, [c]Department of Odontology, [g]Department of Health Education, Federal University of Sergipe, Lagarto, SE, Brazil

[d]Oswaldo Cruz Foundation, Laboratory of Tissue Engineering and Immunopharmacology, Salvador, BA, Brazil

[e] Federal University of Paraíba, João Pessoa, PB, Brazil

*Corre*sponding author:*

Adriana Gibara Guimarães. Department of Health Education, Federal University of Sergipe, Padre Álvares Pitangueira street, nº 248, Downtown, Lagarto/SE. Postal Code: 49400-000 Tel.: +55-79-21056645; Fax: +55-79-3212-6640.

E-mail address: adrianagibara@pq.cnpq.br; adrianagibara@hotmail.com.

ABSTRACT

Background: Oncological pain is one of the most prevalent and difficult-to-treat symptoms in patients with cancer. *p*-cymene (PC) is a monoterpene found in more than 100 different plant species, endowed with various pharmacological properties - particularly antinociceptive.

Hypothesis/Purpose: PC has antinociceptive effect in a model of oncologic pain due to the activation of the descending inhibitory pathway of pain.

Study Design: A pre-clinical, longitudinal, blind and randomized study.

Methods: Male Swiss mice were induced with S180 cells in the right hind paw, then treated daily with PC (12.5, 25 and 50 mg/kg, s.c.) and screened for mechanical hyperalgesia, spontaneous nociception, nociception induced by non-noxious palpation, tumor growth, changes in the neuromuscular function and existence of bone degradation in the tumor area. The effect of PC on Ca^{2+} currents (electrophysiological records), histological and neurochemical changes (immunofluorescence for Fos) were also evaluated.

Results: PC reduced ($p < 0.05$) the mechanical hyperalgesia, the spontaneous ($p < 0.001$) and non-noxious palpation ($p < 0.001$) nociceptions, not changing the tumor development, neuromuscular function or histopathological aspects of the paw affected. PC reduced Fos expression in the spinal cord ($p < 0.001$) and increased this expression in the PAG ($p < 0.05$) and in the NRM ($p < 0.01$). PC decreased the density of calcium channel currents ($p < 0.05$).

Conclusion: These results suggest the antinociceptive effect of PC on oncologic pain, probably acting in both ascending and descending pain pathways, and modulating the calcium channel currents in order to exert its effects.

Keywords: Natural products; Monoterpenes; Antinociceptive; Hyperalgesia; cancer pain.

Abbreviations:

ANOVA: Analysis of variance; BSA: Bovine serum albumin; CGRP: Calcitonin gene-related peptide; DABCO: 1,4-diazabicyclo[2.2.2]octane; DRG: Dorsal root ganglia; ERK1/2: Extracellular signal-regulated kinases 1 and 2; IASP: International Association for the Study of Pain; MAPK: Mitogen-activated protein kinase; NRM: Nucleus raphe magnus; NSAID: Nonsteroidal anti-inflammatory drug; PAG: Periaqueductal gray; PDB: Protein Data Bank; ROI: Region of interest; SEM: Standard error of the mean; TROX-1: N-triazole oxindole; VGCC: Voltage-gated calcium channels.

Introduction

Pain is one of the most common symptoms present in oncologic patients, classified by the World Health Organization (WHO) as a world medical emergency (Gaertner and Schiessl, 2013), due to its high occurrence, complex physiopathology and difficulty of treatment (Gupta et al., 2018). In spite of the existence of several drugs for the treatment of pain, there is many a negative aspect as well, once many of them produce frequent dose-related adverse effects. They often prevent the achievement of the suitable doses necessary for adequate analgesia (Eisenberg and Suzan, 2014), leading to a poor adherence of pharmacotherapy and decreasing quality of life (Ling et al., 2012).

Therefore, natural products derived from plants stand out as a valuable source of therapeutic agents, once they present a number of bioactive chemical compounds associated to the lower risk of side effects, what makes these products possible candidates for the development of new therapies for chronic pain, such as cancer pain (Bahmani et al., 2014). In light of this, monoterpenes and sesquiterpenes represent the major composition of essential oils of aromatic herbs, having several pharmacological properties, particularly the analgesic potential (Gomathi and Manian, 2015; Guimarães et al., 2012, 2014b).

p-Cymene (4-isopropyltoluen; PC) is a monoterpene commonly found in several species of herbs, present in the essential oils of over 100 plant species and naturally occurring in more than 200 kinds of food (orange juice, grapefruit, tangerine, butter, carrots, oregano and most of the spices) (Selvaraj et al., 2002). All over the world, several biological activities have been studied and demonstrated, such as the anti-inflammatory, antinociceptive and analgesic (Bonjardim et al., 2012; de Santana et al., 2015; Quintans-Júnior et al., 2013) and antioxidant activities (de Oliveira

et al., 2015), as well as the immunomodulatory effect (Zhong et al., 2013). Those are a few examples among other studies.

Based on the aforementioned, this study aimed to evaluate the effect of the PC in the therapy of nociception induced by Sarcoma 180 in experimental animals and the mechanisms of action involved, as an alternative for the pain associated with cancer.

Material and methods

Drugs and chemicals

The test compounds used in this study were p-cymene (PC) (1-methyl-4- (1-methylethyl) benzene, 99.7% purity), cremophor, sodium chloride, trypan blue, glycerol, DABCO, glycine and bovine serum albumin (BSA), which were obtained from Sigma-Aldrich (St. Louis, Missouri, USA); morphine and lactated Ringer's solution were purchased from Cristália (São Paulo, São Paulo, Brazil); rabbit anti-Fos k-25 was obtained from Santa Cruz Biotechnology (Dallas, Texas, USA); donkey anti-rabbit Alexa Fluor 488 was purchased from Life Technologies (Carlsbad, California, USA).

Animals

For the experiments, male Swiss mice (between 28-32 g; 2-3 months of age) were used, obtained from the Animal Facilities of the Federal University of Sergipe. All handling procedures and experimental protocols were approved by the Animal Care and Use Committee (CEPA/UFS 03/14) and the adult male Wistar rats (between 200-300 g) were provided by the Animal Center (CEBIO) of the Federal University of Minas Gerais (under protocol number 233/2013), also following the recommendations from the International Association for the Study of Pain (IASP) for the use of animals in pain research (Zimmermann, 1983). The animals were

housed randomly in appropriate cages at 21 ± 2 °C on 12 h light/dark cycle and with free access to food (Purina®, Brazil) and water.

Tumor cell and implantation

Sarcoma 180 (S180) tumor cells were obtained from the Laboratory of Experimental Oncology at the Federal University of Ceará and inoculated in the intraperitoneal region of a maintenance animal. After 10 days of incubation, the mouse was anesthetized, sacrificed and the ascitic fluid was collected from the abdominal cavity. Cells obtained from the ascitic fluid were then analyzed in Neubauer's chamber for the assessment of the percentage of viable cells using Trypan blue solution 1%. A suspension of these tumor cells containing 10^6 cells in 25 µl was implanted in the right hind paw of the mice following a previous protocol (Gouveia et al., 2018; Guimarães et al., 2014a, 2015).

Treatment and behavioral studies

Twenty-four hours after the S180 administrations, the animals (n = 10/group) were treated with vehicle (saline + cremophor 0.4% v/v), PC (12.5, 25 or 50 mg/kg) or morphine (15 mg/kg) via subcutaneous route for 15 consecutive days. During the treatment, behavioral analyses were made on alternating days. The observer responsible for the evaluation was blind to the experimental situation of each animal.

Mechanical hyperalgesia

Mice were evaluated for the sensitivity towards mechanical stimulation by Von Frey's test (electronic anesthesiometer, EFF-301 model, Insight®, Brazil) on the tumor-bearing paw. This stimulation causes a hind limb lifting reflex that corresponds to the paw withdrawal followed by clear movements of flinches (Guimarães et al., 2014a). The intensity of stimulus was obtained by averaging four measurements performed with minimal intervals of 3 min.

Spontaneous and palpation-induced nociception

The animals were placed in scattered boxes and allowed to acclimate during 10 min and evaluated for spontaneous pain through the observation and quantification of flinches performed during a 10-minute period. Afterwards, non-noxious palpation of the paw containing the tumor was performed for 2 minutes, followed by the quantification of flinches for another 2 minutes. Both tests were made following protocols previously established (Sabino et al., 2003).

Movement-evoked pain

The evaluation of the limb use was made through the observation of the animal while walking in a continuous motion in the same boxes scattered, as described by King et al., 2007. This test simulates what occurs among advanced cancer patients, who support body weight on affected limbs. The animals were placed in scattered boxes and allowed to acclimate during 10 min and evaluated for limping and/or guarding behavior of the right (sarcoma-treated) hind limb was rated on the following scale: 0 = complete lack of use, 1 = partial non-use, 2 = limping and guarding, 3 = limping and 4 = normal walking.

Measurement of paw volume

In order to check the effect of PC on tumor growth caused by the S180 implanted in the hind paw of mice, a plethysmometer (Insight®, Brazil) was used, which measured the dislocation of the water column. The paw volume was obtained by averaging three measurements performed before (time zero) and on every other day up to 15 days.

Measurement of forelimb grip strength

Possible changes in neuromuscular function of the animals were also checked by measuring the tension force of limbs using the commercial grip strength meter (Insight®, Brazil) before the

treatment (s.c.) of tumor-free animals with vehicle or PC (12.5, 25 or 50 mg/kg) and 30, 60 and 120 min after treatment (van Riezen and Boersma, 1969). The tension force was obtained by averaging three measurements.

Immunohistochemical studies

The animals (n = 6/group) were injected with PC (50 mg/kg; s.c.), morphine (15 mg/kg; s.c.) or vehicle and ninety minutes later were perfused. The brains and lumbar spinal cords (L4-L6) were collected and cryoprotected for immunofluorescence processed for Fos protein.

Using a cryostat at -20 °C, 20-µm sections were obtained for FOS protein immunofluorescence labeling. Exposure to the reagents started by washing with PBS (phosphate buffer saline) and subsequent exposure to 0.01M glycine diluted in PBS for 10 minutes to reduce tissue autofluorescence caused by exposure to 4% paraformaldehyde, then washed again with PBS. Then, the binding sites for gammaglobulin were blocked with 1% bovine albumin in PBS for 30 minutes. After blocking non-specific reactions, the sections were incubated overnight with rabbit anti-Fos as primary antibodies (1:2000). Afterwards, the sections were incubated for 2h with donkey anti-rabbit Alexa Fluor 594 as secondary antibodies (1:2000).

The spinal cord sections containing neurons positively marked for proteins, to be studied in lamina I of the dorsal horn of the spinal cord, were acquired and classified into regions according to the Paxinos & Watson Atlas, 1997. Then, they were photographed bilaterally using a fluorescence microscope camera (Axioskop 2 plus, Carl Zeiss, Germany). In the photomicrographs, the neurons positively labeled for the protein were quantified; both the arithmetic mean of the number of neurons marked in each region of each animal and the mean of each group were determined.

For quantitative analysis of the markings, a macro (written by the authors) was used in the Image J (National Institutes of Health) computer program, which uses the same level of label intensity to select and count the Fos-positive cells. This protocol was proposed by Brito et al., 2013.

Paw radiography

Animals were sacrificed with the euthanasia method of anesthetic overdose. Thereafter, the right hind paw was removed and fixed in 10% phosphate-buffered formalin for 1 week. After that, the right paws of the animals were radiographed using the Gnatus dental x-ray apparatus, operating at 70 Kvp, 10 mA and time of 0.4 s. The focus-plate distance was 30 cm, with incidence of the radiation focus perpendicular to the plane of the object. The paws were radiographed in anteroposterior incidence. The direct digital image was obtained with a phosphor storage plate as the image receptor (Digora, Soredex, Orion Corporation, Helsinki, Finland). An aluminum penetrometer was used as a densitometric reference. The reading of the sensitized plate was performed on a laser scanner of the very Digora equipment, and the images were manipulated on the software for Windows 1.51. The images were imported into Adobe Photoshop 8.0 image editing software (Adobe Inc. San Jose, CA). In each image, a region of interest (ROI) of 8 x 3 pixel size was selected, located in the central region of the middle finger phalanx in order to prevent the influence of the changes in the scope of the cortical bone. The ROIs were cut and transferred to Image J software version 1.48s (National Institute of Health, Bethesda, MD, http://Rsbinfo.nih.gov/nih-image), where they underwent fractal dimension calculation. In order to remove variations in a medium scale and the brightness scale of the image caused by the difference in object thickness and radiation exposure, the trimmed ROI was duplicated and the duplicate image was blurred with a Gaussian filter (kernel size = 35). The

blurred image was then subtracted from the original image and the resulting image was converted to the binarization threshold at the gray value of 128, so that the segmented objects approximate the bone trabecular pattern. Finally, the image was skeletonized for fractal analysis. The fractal dimension of the skeletized image was calculated using the box-counting function in the "analyze" menu of the Image J software. The box widths were 2, 3, 4, 6, 8, 12, 16, 32 and 64 pixels.

Histophatological analysis

Different groups of animals (n = 8/group) were sacrificed by excess sedation on the 15th day after sarcoma inoculation. The paws were then collected, fixed and stained for posterior optical microscopy screening for histopathological characteristics of the tumor, as described by King et al., 2007.

DRG culture

In order to evaluate the effect of PC on the Ca^{2+} current, the dorsal root ganglia cells (DRG) from adult male Wistar rats were used, which were obtained by the dissection protocol adapted from Sleigh et al., 2016.

Whole-cell voltage-clamp and calcium imaging

The electrophysiological records of DRGs were obtained using the patch-clamp technique in the whole cell under voltage-clamp modality for the measurements of the calcium currents following the established protocol (de Menezes-Filho et al., 2014).

Docking studies

The intermolecular interactions between PC and the various subtypes of voltage-gated calcium channels (VGCC) were evaluated through docking studies, using as ligands: PC, nicardipine, ω-agatoxin IVA, ω-conotoxin GVIA and N-triazole oxindole (TROX-1). The macromolecules used

were obtained from the Protein Data Bank, which were: CaV1 (L-type) calcium channels (PDB ID 5GJV), CaV2.1 (P/Q-type) calcium channels (PDB ID 3BXK), CaV2.2 (N-type) calcium channels (PDB ID 3DVE) and CaV2.3 (R-type) calcium channels (PDB ID 3BXL). The ligands were subjected to molecular anchoring using molecular docking algorithm MolDock (Thomsen and Christensen, 2006).

Statistical analysis

The data obtained were evaluated by analyses of variance (ANOVA) in means ± standard error of the mean (SEM) of one- and two-way trials, followed by Tukey's test. For the limb use and paw radiography, the test of Kruskal-Wallis was applied, followed by Dunn's test. In all cases, differences were considered significant if $p < 0.05$, using the Graph Pad Prism (v 4.00) software (San Diego, CA, USA). The percent of inhibition was determined using the following formula: Inhibition% (PI) = 100*(control - experiment)/control, with the data obtained from the area under the curve (AUC).

Results and discussion

On the day after the induction of the intraplantar sarcoma 180 tumor cells, the animals began to be evaluated on alternate days until the fifteenth day. The mice did not present an evident hyperalgesic behavior until the ninth day, as a result of the tumor development process, when using von Frey digital analgesimeter. From the eleventh day of observation onward, this difference was statistically significant between the Vehicle and the Sham groups ($p < 0.001$) (Fig. 1.A), demonstrating the hypernociception induced by such model.

The *p*-cymene (PC) in the dose of 50 mg/kg was capable to revert the hyperalgesic chart from the eleventh to the fifteenth day ($p < 0.05$) with an average inhibition percentage of 60.4%, such

as morphine ($p < 0.01$, days 11 to 13; $p < 0.001$, 15th day), which also promoted a reduction in the animal sensitization (Fig. 1.A). After the fifteenth day, continuing the experiment was impracticable due to tumor development.

In the test of spontaneous nociception, the Sham group showed a significant difference from the vehicle group from the ninth day forward ($p < 0.001$). All the PC doses maintained the basal behavior of the mice until the thirteenth day ($p < 0.001$). Furthermore, the 50 mg/kg of PC promoted a significant inhibition percentage of 100% of this behavior, similar to morphine (99.2%) (Fig. 1.B).

Evaluating the nociception caused by noxious palpation, all the groups presented a statistical significance when compared to vehicle group ($p < 0.001$) with inhibition percentages ranging from 75.8% and 72.6% at the lower doses (12.5 and 25 mg/kg, respectively) to 99.2% at the highest dose tested (50 mg/kg) (Fig. 1.C).

[INSERT FIG. 1]

Each experiment mimicked a kind of pain presented by patients with neoplasia, as hyperalgesia, spontaneous nociception and allodynia. These have been associated with the sensitization of specific fibers, such as an increase in the suprathreshold response of C and A-δ in hyperalgesia, a sensitization of C-fiber nociceptors in spontaneous nociception and allodynia through a lower threshold of the A-β fibers. The findings herein reported corroborate with the results described by Guimarães et al., 2014a.

Previous studies demonstrated that PC presents a proven anti-inflammatory and analgesic pharmacological profile in models of acute and orofacial pain (Bonjardim et al., 2012; de

Santana et al., 2015; Santana et al., 2011), but they lacked information about its effect on chronic pain, such as cancer pain. This study showed that PC was able to attenuate the nociceptive effects against oncological factors.

The effects of PC on tumor development were assessed as for the paw volume, which they were shown not to significantly reduce. The movement-evoked pain test did not show significant inhibition in the reduction of paw utilization by the mice (supplementary material). However, another study (Li et al., 2016) demonstrated that PC has the antitumor effect due to the modulation of ERK1/2 and p38 MAPK signal pathways in tumor cells.

It was also assessed that the mice in use of PC showed no difference in the intensity of grip strength when compared to the vehicle group (data not shown), accounting for the absence of any myorelaxant effect provided by the monoterpene under test. In fact, Quintans et al., 2013, showed that PC was not able to interfere in the motor performance in mice.

The histopathological analysis of the paws with Sarcoma 180 treated with vehicle (cremophor + saline) removed post-mortem revealed neoplasia, characterized by the proliferation of polygonal, ovoid, round or rhabdoid tumor cells, organized in fuzzy sheets, at times compact and at times loosely arranged. The tumor component was bordering the bone tissue and at times coming into contact with some points of infiltration. Perineural invasion and area of coagulative necrosis were observed. Inflammatory lymphocytic infiltration of variable intensity and some mitotic Fig.s were also visible (Fig. 2.A). No differences were observed in the morphological pattern of the tumors developed in the different groups studied, regardless of the treatment.

[INSERT FIG. 2]

Histopathology of the paws containing Sarcoma 180 and treated with PC (50 mg/kg) removed post-mortem revealed neoplasia characterized by the proliferation of polygonal, ovoid, round or rhabdoid tumor cells, organized in diffuse sheets, at times compact and at times loosely arranged. The tumor component often invaded and dissociated both bundles of skeletal striated muscle fibers and the dermal adipose panicle, at times coming in contact with the bone tissue presenting a few spots of infiltration. Individually, the parenchymal cells exhibited moderated cellular pleomorphism, while the nuclei at times presented dense chromatin and at other times thinly dispersed and one to two prominent nucleoli. Extensive areas of necrosis were also evidenced, as well as interstitial edema, probably due to lymphocytic inflammatory infiltration of variable intensity and some mitotic Fig.s, some of them atypical (Fig. 2.B).

Regarding the effect of PC on the histopathological characteristics of the tumor, a previously published study has shown that essential oils consisting of PC, such as oregano oil (*Origanum vulgare*), present high levels of cytotoxicity against animal permanent cell lines, including two derivatives of human cancers (Sivropoulou et al., 1996). Nonetheless, no significant difference was found between the tumors of the non-treatment group and the group under treatment with PC.

Through radiological and fractal analysis, it was not possible to verify bone lesions associated with the presence of the tumor, demonstrating no evidence that sarcoma 180 is able to invade bone regions within 15 days (supplementary material).

On the fifteenth day, the animals of the vehicle group presented a significant increase ($p < 0.001$) in the number of positive Fos neurons in the lumbar spinal cord (L4-L6) lamina 1 when compared to the Sham group. PC (50 mg/kg) and morphine (15 mg/kg) groups reduced this neuronal labeling ($p < 0.001$) (Fig. 3).

[INSERT FIG. 3]

There was also a significant increase in active neurons in the periaqueductal gray (PAG) (Fig. 4A.1) in the animals treated with PC (50 mg/kg) ($p < 0.05$) and morphine ($p < 0.001$) as well as in the nucleus raphe magnus (NRM) ($p < 0.01$ and 0.001, respectively) (Fig. 4A.2).

[INSERT FIG. 4]

The results corroborate a previous study, which showed that some substances with analgesic effect have the capability to increase the expression of Fos protein in regions that comprise the descending pathway of pain, such as PAG and NRM, and consequently decrease this expression in the spinal cord (Santos et al., 2018). This pathway is an important site of action of several pharmacological classes related to the analgesic effect, such as opiates, cannabinoids, nonsteroidal anti-inflammatory drugs (NSAIDs) and serotonin/norepinephrine reuptake blockers (Ossipov et al., 2010).

In fact, previous studies had demonstrated that PC modulates opioid receptors non-selectively (de Santana et al., 2015; Santana et al., 2011). As it is known, when an opioid agonist binds to a G-protein-coupled opioid receptor, it promotes intracellular alterations, what leads to the activation of potassium conductance and an inhibition of calcium conductance, hyperpolarizing the cell and reducing the pain (Pathan and Williams, 2012). Although there are already reports about the effect of PC on potassium channels (Silva et al., 2015), no study shows its effect on calcium channels. Then, in order to better understand the pathways of action of PC to reduce the

pain, how this compound would act in voltage-gated calcium channel (VGCC) currents was analyzed.

Fig. 5A shows representative current traces of I_{Ca}, in dorsal root ganglia (DRG) neurons in control situation (top panel) and after 4.0 min (middle panel) and 7.5 min (bottom panel) of perfusion with PC (200 μM). As it can be seen, PC significantly decreased the I_{Ca} peak. Time course of the PC effect (200 μM) on the I_{Ca} density is shown in Fig. 5B. Interestingly, PC reduced the I_{Ca} from -0.97 ± 0.36 pA/pF to 0.067 ± 0.002 pA/pF (99.8%, Fig. 5C, $p < 0.05$, n = 6-10).

[INSERT FIG. 5]

Modulation of VGCC currents is a mechanism already established by mediating the painful signs in primary afferent neurons (Zamponi et al., 2009) and dorsal horn neurons of the spinal cord (Park and Luo, 2010). In addition, VGCCs contribute to the modulation of sensory signals in the ascending and descending pathways, being potential targets for the management of chronic pain.

When PC was complexed with the CaV1, CaV2.1, CaV2.2 and CaV2.3 calcium channels, we found negative energy values of -60.118, -59.60, -49.55 and -59.95 kcal/mol, respectively, suggesting that the binding between the targets is favorable and possibly occurs, since the more negative the energy values are, the more favorable the interaction is (Du et al., 2016). Fig. 6 reports the ligand maps calculated with the best conformations and all the binding energy values in relation to their receptors. Some results were found close to those presented from the control, as it can be seen in the complex of CaV2.2 calcium channels and ω-conotoxin GVIA (binding energy -48.72 kcal/mol). In fact, these VGCCs, mainly CaV2.2, are found in presynaptic

terminals and play an important role in pain neurotransmitter release such as CGRP, substance P, and glutamate (Lee, 2013).

[INSERT FIG. 6]

Corroborating the above mentioned, PC was able to significantly reduce the calcium current density. The straight inhibition of calcium channels by exogenous substances may possibly induce antinociception by itself (Freitas et al., 2018). Also, it is one of the action mechanisms of some existing drugs currently used for the treatment of chronic pain, such as gabapentinoids (Catterall and Swanson, 2015).

Conclusions

Thus, the results of this study clearly demonstrated the antinociceptive effect of PC in the oncological pain model induced by S180, in addition to the properties presented by the drug, such as the neuromodulatory, and its action in calcium current. It is also suggested to act on the ascending and descending pathways of pain inhibition and also to become a possible candidate for the treatment of cancer pain.

Acknowledgment

We would like to thank teachers Pollynne Holanda and Abilio Borghi for the grammar review of the manuscript.

Conflict of interest

The authors declare no competing financial interest.

Funding sources

We thank for the grants from the Foundation for Research and Technological Innovation Support of the State of Sergipe (Fundação de Apoio à Pesquisa e Inovação Tecnológica do Estado de Sergipe/ FAPITEC/SE), the National Council of Technological and Scientific Development (Conselho Nacional de Desenvolvimento Científico e Tecnológico/CNPq/Brazil 449667/2014-6) and Coordenação de Aperfeiçoamento de Pessoal de Nível Superior (CAPES/Brazil).

References

Bahmani, M., Shirzad, H., Majlesi, M., Shahinfard, N., Rafieian-Kopaei, M., 2014. A review study on analgesic applications of Iranian medicinal plants. Asian Pac. J. Trop. Med. 7S1, S43-53. https://doi.org/10.1016/S1995-7645(14)60202-9

Bonjardim, L.R., Cunha, E.S., Guimarães, A.G., Santana, M.F., Oliveira, M.G.B., Serafini, M.R., Araújo, A.A.S., Antoniolli, A.R., Cavalcanti, S.C.H., Santos, M.R.V., Quintans-Júnior, L.J., 2012. Evaluation of the anti-inflammatory and antinociceptive properties of p-cymene in mice. Z. Naturforschung C J. Biosci. 67, 15–21. https://doi.org/10.5560/ZNC.2012.67c0015

Brito, R.G., Santos, P.L., Prado, D.S., Santana, M.T., Araújo, A.A.S., Bonjardim, L.R., Santos, M.R.V., de Lucca Júnior, W., Oliveira, A.P., Quintans-Júnior, L.J., 2013. Citronellol reduces orofacial nociceptive behaviour in mice - evidence of involvement of retrosplenial cortex and periaqueductal grey areas. Basic Clin. Pharmacol. Toxicol. 112, 215–221. https://doi.org/10.1111/bcpt.12018

Catterall, W.A., Swanson, T.M., 2015. Structural Basis for Pharmacology of Voltage-Gated Sodium and Calcium Channels. Mol. Pharmacol. 88, 141–150. https://doi.org/10.1124/mol.114.097659

de Menezes-Filho, J.E.R., Gondim, A.N.S., Cruz, J.S., de Souza, A.A., Santos, J.N.A. dos, Conde-Garcia, E.A., de Sousa, D.P., Santos, M.S., de Oliveira, E.D., de Vasconcelos, C.M.L., 2014. Geraniol Blocks Calcium and Potassium Channels in the Mammalian Myocardium: Useful Effects to Treat Arrhythmias. Basic Clin. Pharmacol. Toxicol. 115, 534–544. https://doi.org/10.1111/bcpt.12274

de Oliveira, T.M., de Carvalho, R.B.F., da Costa, I.H.F., de Oliveira, G.A.L., de Souza, A.A., de Lima, S.G., de Freitas, R.M., 2015. Evaluation of p-cymene, a natural antioxidant. Pharm. Biol. 53, 423–428. https://doi.org/10.3109/13880209.2014.923003

de Santana, M.F., Guimarães, A.G., Chaves, D.O., Silva, J.C., Bonjardim, L.R., de Lucca Júnior, W., Ferro, J.N. de S., Barreto, E. de O., dos Santos, F.E., Soares, M.B.P., Villarreal, C.F., Quintans, J. de S.S., Quintans-Júnior, L.J., 2015. The anti-hyperalgesic and anti-inflammatory profiles of p-cymene: Evidence for the involvement of opioid system and cytokines. Pharm. Biol. 53, 1583–1590. https://doi.org/10.3109/13880209.2014.993040

Du, X., Li, Y., Xia, Y.-L., Ai, S.-M., Liang, J., Sang, P., Ji, X.-L., Liu, S.-Q., 2016. Insights into Protein–Ligand Interactions: Mechanisms, Models, and Methods. Int. J. Mol. Sci. 17. https://doi.org/10.3390/ijms17020144

Eisenberg, E., Suzan, E., 2014. Drug combinations in the treatment of neuropathic pain. Curr. Pain Headache Rep. 18, 463. https://doi.org/10.1007/s11916-014-0463-y

Freitas, A.C.N., Peigneur, S., Macedo, F.H.P., Menezes-Filho, J.E., Millns, P., Medeiros, L.F., Arruda, M.A., Cruz, J., Holliday, N.D., Tytgat, J., Hathway, G., de Lima, M.E., 2018. The Peptide PnPP-19, a Spider Toxin Derivative, Activates μ-Opioid Receptors and Modulates Calcium Channels. Toxins 10, 43. https://doi.org/10.3390/toxins10010043

Gaertner, J., Schiessl, C., 2013. Cancer pain management: what's new? Curr. Pain Headache Rep. 17, 328. https://doi.org/10.1007/s11916-013-0328-9

Gomathi, R., Manian, S., 2015. Analgesic and acetylcholinesterase inhibition potential of polyphenols from Scolopia crenata (Flacourtiaceae): An endemic medicinal plant of India. Ind. Crops Prod. 73, 134–143. https://doi.org/10.1016/j.indcrop.2015.03.090

Gouveia, D.N., Costa, J.S., Oliveira, M.A., Rabelo, T.K., Silva, A.M. de O.E., Carvalho, A.A., Miguel-Dos-Santos, R., Lauton-Santos, S., Scotti, L., Scotti, M.T., Santos, M.R.V.D., Quintans-Júnior, L.J., Albuquerque Junior, R.L.C.D., Guimarães, A.G., 2018. α-Terpineol reduces cancer pain via modulation of oxidative stress and inhibition of iNOS. Biomed. Pharmacother. Biomedecine Pharmacother. 105, 652–661. https://doi.org/10.1016/j.biopha.2018.06.027

Guimarães, A.G., Oliveira, M.A., Alves, R. dos S., Menezes, P. dos P., Serafini, M.R., Araújo, A.A. de S., Bezerra, D.P., Quintans Júnior, L.J., 2015. Encapsulation of carvacrol, a monoterpene present in the essential oil of oregano, with β-cyclodextrin, improves the pharmacological response on cancer pain experimental protocols. Chem. Biol. Interact. 227, 69–76. https://doi.org/10.1016/j.cbi.2014.12.020

Guimarães, A.G., Quintans, J.S.S., Quintans, L.J., 2012. Monoterpenes with analgesic activity--a systematic review. Phytother. Res. PTR 27, 1–15. https://doi.org/10.1002/ptr.4686

Guimarães, A.G., Scotti, L., Scotti, M.T., Mendonça Júnior, F.J.B., Melo, N.S.R., Alves, R.S., De Lucca Júnior, W., Bezerra, D.P., Gelain, D.P., Quintans Júnior, L.J., 2014a. Evidence for the involvement of descending pain-inhibitory mechanisms in the attenuation of cancer pain by carvacrol aided through a docking study. Life Sci. 116, 8–15. https://doi.org/10.1016/j.lfs.2014.08.020

Guimarães, A.G., Serafini, M.R., Quintans-Júnior, L.J., 2014b. Terpenes and derivatives as a new perspective for pain treatment: a patent review. Expert Opin. Ther. Pat. 24, 243–265. https://doi.org/10.1517/13543776.2014.870154

Gupta, A., Tankha, P., Ahmad, M., 2018. Chronic Pain Management and Maxillofacial Surgery, in: Perioperative Assessment of the Maxillofacial Surgery Patient. Springer, Cham, pp. 359–371. https://doi.org/10.1007/978-3-319-58868-1_26

King, T., Vardanyan, A., Majuta, L., Melemedjian, O., Nagle, R., Cress, A.E., Vanderah, T.W., Lai, J., Porreca, F., 2007. Morphine treatment accelerates sarcoma-induced bone pain, bone loss, and spontaneous fracture in a murine model of bone cancer. Pain 132, 154–168. https://doi.org/10.1016/j.pain.2007.06.026

Lee, S., 2013. Pharmacological Inhibition of Voltage-gated Ca(2+) Channels for Chronic Pain Relief. Curr. Neuropharmacol. 11, 606–620. https://doi.org/10.2174/1570159X11311060005

Li, J., Liu, C., Sato, T., 2016. Novel Antitumor Invasive Actions of p-Cymene by Decreasing MMP-9/TIMP-1 Expression Ratio in Human Fibrosarcoma HT-1080 Cells. Biol. Pharm. Bull. 39, 1247–1253. https://doi.org/10.1248/bpb.b15-00827

Ling, C., Lui, L.Y.Y., So, W.K.W., 2012. Do educational interventions improve cancer patients' quality of life and reduce pain intensity? Quantitative systematic review. J. Adv. Nurs. 68, 511–520. https://doi.org/10.1111/j.1365-2648.2011.05841.x

Ossipov, M.H., Dussor, G.O., Porreca, F., 2010. Central modulation of pain. J. Clin. Invest. 120, 3779–3787. https://doi.org/10.1172/JCI43766

Park, J.F., Luo, Z.D., 2010. Calcium channel functions in pain processing. Channels 4, 510–517. https://doi.org/10.4161/chan.4.6.12869

Pathan, H., Williams, J., 2012. Basic opioid pharmacology: an update. Br. J. Pain 6, 11–16. https://doi.org/10.1177/2049463712438493

Quintans, J. de S.S., Menezes, P.P., Santos, M.R.V., Bonjardim, L.R., Almeida, J.R.G.S., Gelain, D.P., Araújo, A.A. de S., Quintans-Júnior, L.J., 2013. Improvement of p-cymene antinociceptive and anti-inflammatory effects by inclusion in β-cyclodextrin. Phytomedicine Int. J. Phytother. Phytopharm. 20, 436–440. https://doi.org/10.1016/j.phymed.2012.12.009

Quintans-Júnior, L., Moreira, J.C.F., Pasquali, M.A.B., Rabie, S.M.S., Pires, A.S., Schröder, R., Rabelo, T.K., Santos, J.P.A., Lima, P.S.S., Cavalcanti, S.C.H., Araújo, A.A.S., Quintans, J.S.S., Gelain, D.P., 2013. Antinociceptive Activity and Redox Profile of the Monoterpenes (+)-Camphene, p-Cymene, and Geranyl Acetate in Experimental Models. ISRN Toxicol. 2013. https://doi.org/10.1155/2013/459530

Sabino, M.A.C., Luger, N.M., Mach, D.B., Rogers, S.D., Schwei, M.J., Mantyh, P.W., 2003. Different tumors in bone each give rise to a distinct pattern of skeletal destruction, bone cancer-related pain behaviors and neurochemical changes in the central nervous system. Int. J. Cancer 104, 550–558. https://doi.org/10.1002/ijc.10999

Santana, M.F., Quintans-Júnior, L.J., Cavalcanti, S.C.H., Oliveira, M.G.B., Guimarães, A.G., Cunha, E.S., Melo, M.S., Santos, M.R.V., Araújo, A.A.S., Bonjardim, L.R., 2011. p-Cymene reduces orofacial nociceptive response in mice. Rev. Bras. Farmacogn. 21, 1138–1143. https://doi.org/10.1590/S0102-695X2011005000156

Santos, P.L., Brito, R.G., Matos, J.P.S.C.F., Quintans, J.S.S., Quintans-Júnior, L.J., 2018. Fos Protein as a Marker of Neuronal Activity: a Useful Tool in the Study of the Mechanism of Action of Natural Products with Analgesic Activity. Mol. Neurobiol. 55, 4560–4579. https://doi.org/10.1007/s12035-017-0658-4

Selvaraj, M., Pandurangan, A., Seshadri, K.S., Sinha, P.K., Krishnasamy, V., Lal, K.B., 2002. Comparison of mesorporous A1-MCM-41 molecular sieves in the production of p-cymene for isopropylation of toluene. J. Mol. Catal. Chem. 186, 173–186. https://doi.org/10.1016/S1381-1169(02)00134-6

Silva, M.T.M., Ribeiro, F.P.R.A., Medeiros, M.A.M.B., Sampaio, P.A., Silva, Y.M.S., Silva, M.T.A., Quintans, J.S.S., Quintans-Júnior, L.J., Ribeiro, L.A.A., 2015. The Vasorelaxant Effect of p-Cymene in Rat Aorta Involves Potassium Channels. Sci. World J. 2015. https://doi.org/10.1155/2015/458080

Sivropoulou, A., Papanikolaou, E., Nikolaou, C., Kokkini, S., Lanaras, T., Arsenakis, M., 1996. Antimicrobial and Cytotoxic Activities of Origanum Essential Oils. J. Agric. Food Chem. 44, 1202–1205. https://doi.org/10.1021/jf950540t

Sleigh, J.N., Weir, G.A., Schiavo, G., 2016. A simple, step-by-step dissection protocol for the rapid isolation of mouse dorsal root ganglia. BMC Res. Notes 9, 82. https://doi.org/10.1186/s13104-016-1915-8

Thomsen, R., Christensen, M.H., 2006. MolDock: a new technique for high-accuracy molecular docking. J. Med. Chem. 49, 3315–3321. https://doi.org/10.1021/jm051197e

van Riezen, H., Boersma, L., 1969. A new method for quantitative grip strength evaluation. Eur. J. Pharmacol. 6, 353–356. https://doi.org/10.1016/0014-2999(69)90197-6

Zamponi, G.W., Lewis, R.J., Todorovic, S.M., Arneric, S.P., Snutch, T.P., 2009. Role of voltage-gated calcium channels in ascending pain pathways. Brain Res. Rev. 60, 84–89. https://doi.org/10.1016/j.brainresrev.2008.12.021

Zhong, W., Chi, G., Jiang, L., Soromou, L.W., Chen, N., Huo, M., Guo, W., Deng, X., Feng, H., 2013. p-Cymene modulates in vitro and in vivo cytokine production by inhibiting MAPK and NF-κB activation. Inflammation 36, 529–537. https://doi.org/10.1007/s10753-012-9574-y

Zimmermann, M., 1983. Ethical guidelines for investigations of experimental pain in conscious animals. Pain 16, 109–110. https://doi.org/10.1016/0304-3959(83)90201-4

Figure legnds

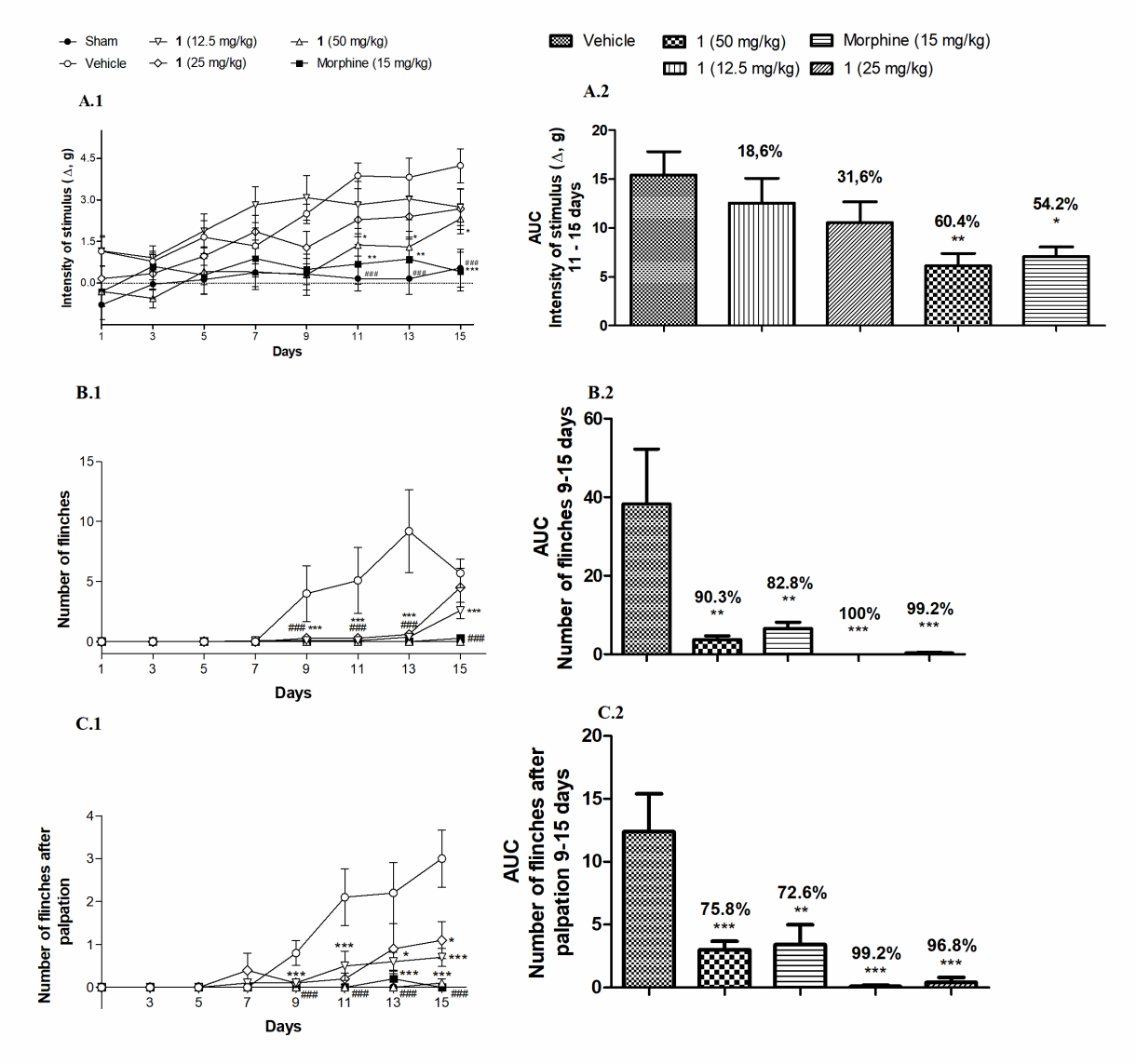

Fig. 1. *p*-cymene (PC) effect (12.5 to 50 mg/kg, s.c.) on mechanical hyperalgesia (A), spontaneous (B) and palpation-induced nociception (C) induced by S180. *p < 0.05, **p < 0.01 and ***p < 0.001 vs. the control group; ###p < 0.001 vs. sham (ANOVA followed by Tukey's test).

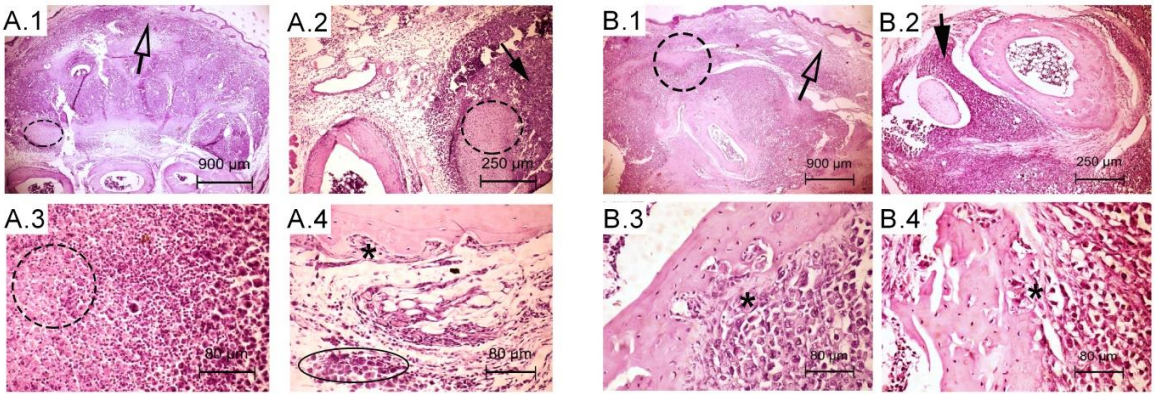

Fig. 2. Histopathological analysis through light microscopy in mice carrying intraplantar sarcoma 180 and treated with vehicle (saline + cremophor) (A) and *p*-cymene (PC) (B) subcutaneously for 15 days. Staining with hematoxylin and eosin. A.1, B.1: 40x magnification; A.2, B.2: 100x magnification; A.3, A.4, B.3, B.4: 400x magnification. The solid line ellipse shows the variety of cell types presented by the tumor. Several points of coagulative necrosis are shown by dotted ellipses. Regions in which tumor cells come into contact with bone tissue are marked with an asterisk. Empty arrows demonstrate several areas of interstitial edema and areas of lymphocytic infiltrate are pointed by filled arrows.

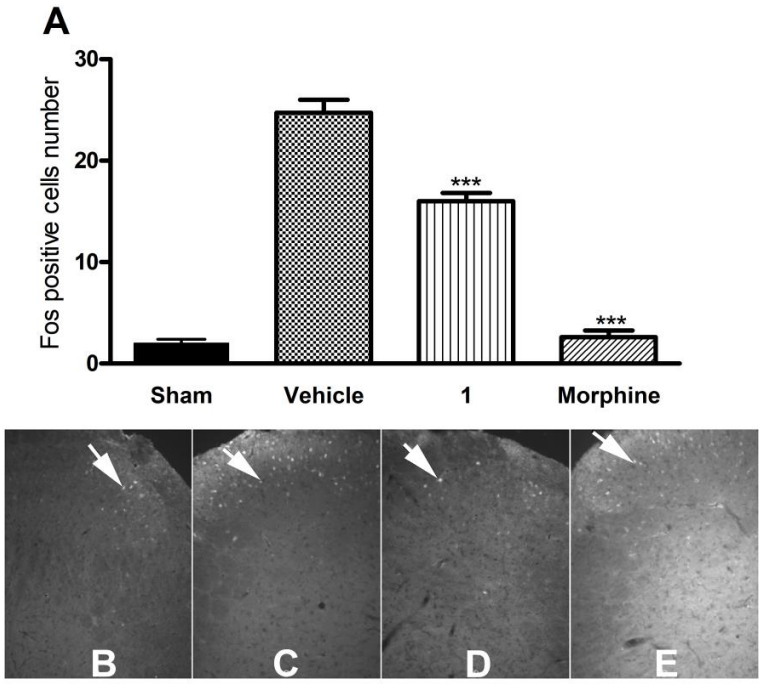

Fig. 3. Effect of p-cymene (PC) (50 mg/kg, s.c) on the activation of Fos positive neurons in lamina I of the lumbar cord. (A) The values were expressed as mean ± SEM (n = 6/group), ***p < 0.001 vs. control group (one-way ANOVA followed by Tukey's test). Immunofluorescence for Fos protein in neurons (arrows) in lamina 1 of the lumbar cord in the sham (B), vehicle (C), PC (D) and morphine (E) groups.

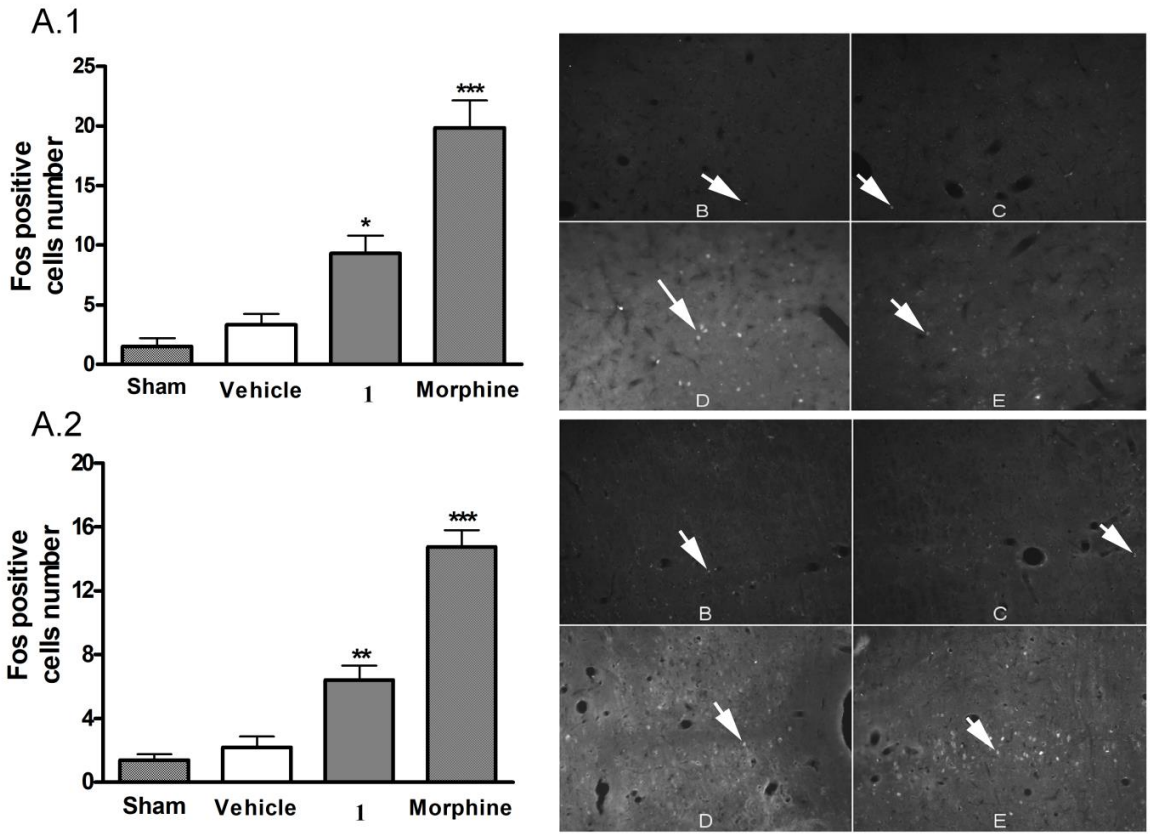

Fig. 4. Effect of *p*-cymene (PC) (50 mg/kg, s.c) on the activation of Fos positive neurons in periaqueductal gray (PAG) (A.1) and nucleus raphe magnus (NRM) (A.2). (A) The values were expressed as mean ± SEM (n = 6/group), *p < 0.05, *p < 0.01, and ***p < 0.001 vs. control group (one-way ANOVA followed by Tukey's test). Immunofluorescence for Fos protein in neurons (arrows) of PAG and NRM in sham (B), vehicle (C), PC (D) and morphine (E) groups.

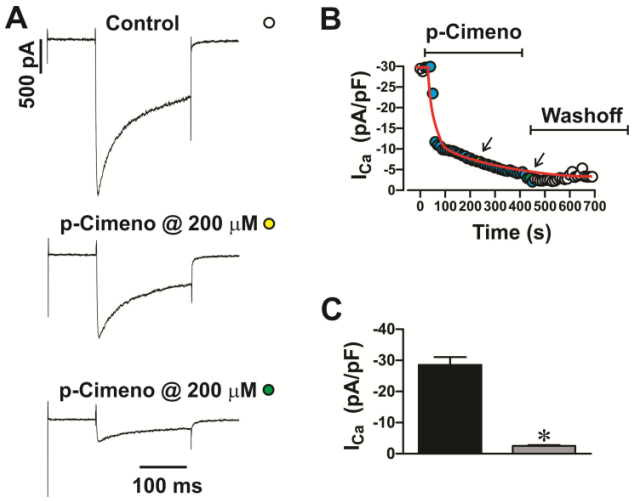

Fig. 5. Effect of *p*-cymene (PC) on I_{Ca} peak in dorsal root ganglia. A) Representative traces of I_{Ca} obtained in control (top), and after 4.0 min (middle) and 7.5 min (bottom) of perfusion with PC (200 μM). Cells were kept at a holding potential of -90 mV, then depolarized to -10 mV (for 200 msec.) at 20-second intervals. B) Time course for 200 μM PC effect on I_{Ca} density. C) Averaged effect of PC on I_{Ca} amplitude (n = 6-10, *$p < 0.05$).

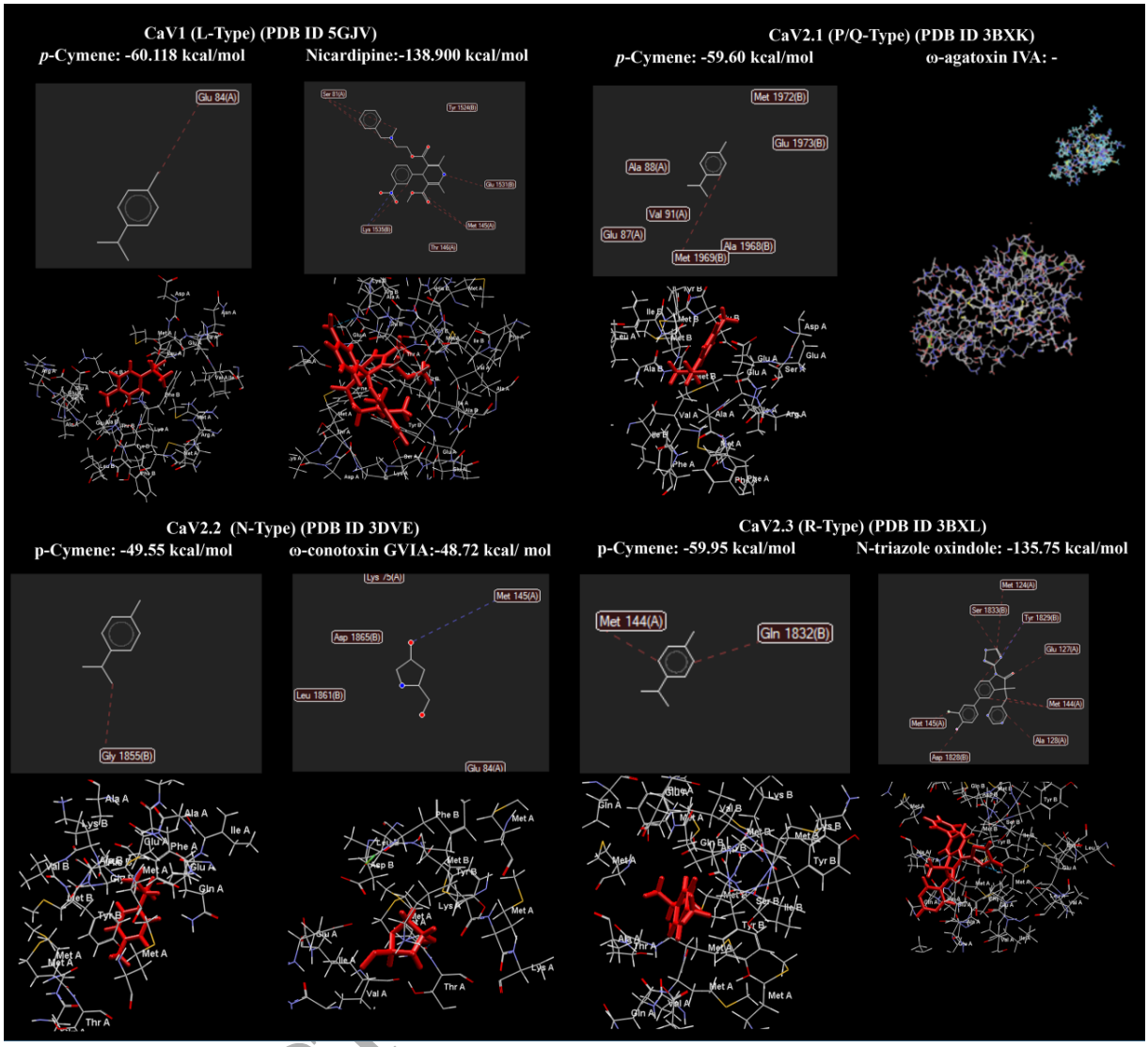

Fig. 6. Ligand Maps with the respective binding energies. Blue lines – hydrogen bonds, red lines – steric interactions.

Graphical Abstract